

# Effect of thermophoresis on fog droplet deposition on low pressure steam turbine guide blades

D. J. Ryley\* and J. B. Davies†

Deposition of droplets in the sub-micron size range, when discouraged by thermophoresis forces, has been studied by a simulation method employing uranine particles entrained in air and flowing through a cascade of full-sized low-pressure steam turbine blades. The particles, generated by a Collison atomiser, had a mass-median diameter range of 0.05–0.25  $\mu\text{m}$ . The test blades were internally heated using hot air and had an output of 600 W/m<sup>2</sup> of swept surface. Circumferential tape around their surfaces provided a reception medium for the particles, the deposition density variation of which was found by fluorimetry. Prediction of the deposition on an unheated blade using the method of C. N. Davies showed acceptable agreement with the experimental results. The simulation method was validated by showing that the relevant non-dimensional numbers, Schmidt and Reynolds, can be acceptably matched for the air/particle and the steam/droplet cases. Tests on the heated blade showed that the deposition was reduced by 30–90% of the corresponding value for the unheated blade. The extent of the reduction decreased with particle size decrease

**Key words:** *steam turbines, turbine blades, thermophoresis*

Erosion in wet steam turbines is caused by the impact of large ('coarse') water drops on the convex side of the inlet edge of the rotor blades. These droplets arise from fragmentation, at the trailing edge of the guide blades, of water previously deposited on these blades by the wet steam during transit. As the first appearance of water in the steam is in the form of fog droplets, some of these droplets must alight on the guide blade surface, to be propelled to the exit edge and there be broken up to provide the coarse water causing the damage.

The first operation, ie the initial deposition of the fog droplets, has been studied at some length, both theoretically and experimentally, in the Wet Steam Laboratory at the University of Liverpool. When the original research programme was planned in 1966, the view was taken that experiments conducted directly with nucleated steam would prove unprofitable since there was no way in which the distribution of deposition over the blade surface could be ascertained with confidence. Hence a simulation method was adopted using fluorescein particles entrained in air<sup>1</sup>. These particles were generated in the size range 0.01–1.0  $\mu\text{m}$  diameter corresponding to that of grown turbine fog droplets; they were

entrained in air which was supplied to a cascade of full-size steam turbine guide blade profiles mounted in a specially designed tunnel. The distribution of deposition was found by using a metal foil reception strip wrapped around the blade surface, sections of which were subsequently tested for deposition density using fluorimetric methods. This apparatus was first employed to determine the deposition of fog for a turbine running under normal design conditions<sup>2</sup> and subsequently for a turbine running under part load conditions<sup>3</sup>. In both cases good agreement was shown between the deposition measured experimentally and that predicted from theory.

It was realised that the blades were sufficiently large to permit internal channels for a heating medium and that, if blade heating was employed on the production turbine, thermophoretic forces would act upon any fog droplets within the thermal boundary layer and discourage deposition. In this way the erosion process might be halted or at least impeded. Subject to certain reservations to be explored later, it was possible to study this problem using the simulation method and these studies form the subject of this paper.

## Apparatus

The original apparatus was extended to provide internal blade heating. The basic form of the apparatus has been described elsewhere and only the modifications for blade heating will be described here.

\* Department of Mechanical Engineering, University of Liverpool, P.O. Box 147, Liverpool L69 3BX, UK

† The University of Sierra Leone, Fourah Bay College, Freetown, Sierra Leone. Formerly a Research Student in the Department of Mechanical Engineering at the University of Liverpool

Received 2 February 1983 and accepted for publication on 25 April 1983

Fig 1(a) shows the heating system. The gas heater supplied hot air to a mixing manifold from which three adjacent heated blades were supplied via a set of 12 (4 per blade) insulated 'flexflyte' tubes made of neoprene-coated woven fibreglass reinforced with galvanised spring steel. The air temperature was controlled by adjusting the gas supply, varying the air fan speed and manipulating the manifold bleed valve. The total volume flow of air through each blade was about 340 ml/s and limitations on the tube material restricted the temperature on the swept faces of the blades to about 50 °C. Fig 1(b) shows the extent of the interior heating chambers, all of which may be independently heated. Heating air entry tubes mounted on the assembled blade are shown in Fig 2. The centre part of the working profile is made of aluminium. Twenty-five copper-constantan thermo-junctions were centrally placed around the profile periphery. The heat entry and exit pipes were made of bakelite. The rate of heat dissipation from the working surface was about 600 W/m<sup>2</sup> and kept approximately constant throughout the tests. Throughout these tests all heating chambers were in use.

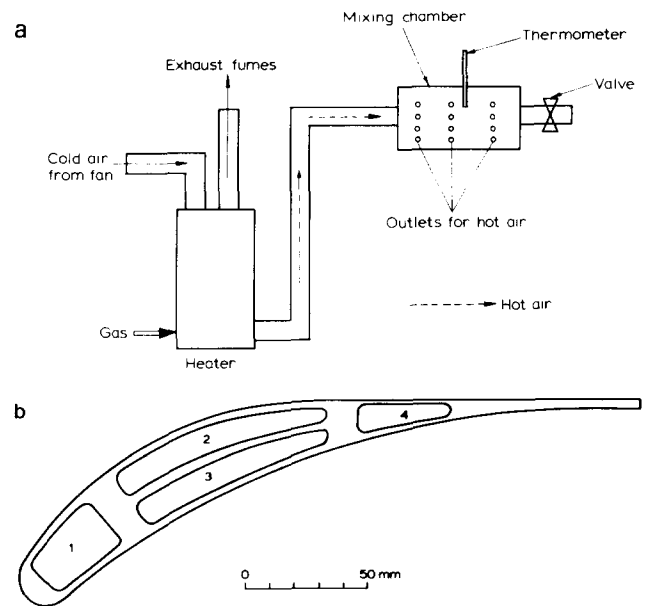


Fig 1(a) Schematic layout of heating system (b) Cross section of interior heating chambers. All passages are single pass

### Notation

|               |  |
|---------------|--|
| $c$           | Blade chord                            |
| $C$           | Particle concentration                 |
| $d$           | Particle diameter ( $= 2r$ )           |
| $D$           | Particle diffusivity                   |
| $E$           | Cunningham correction                  |
| $F$           | Thermal velocity coefficient           |
| $H$           | Shape factor                           |
| $K$           | Deposition velocity                    |
| $k$           | Thermal conductivity                   |
| $l$           | Molecular mean free path               |
| $N$           | Particle flux density                  |
| $\dot{q}$     | Heat input per unit area               |
| $R$           | Blade nose radius                      |
| $r$           | Particle radius                        |
| $s$           | Stopping distance                      |
| $T$           | Temperature                            |
| $t$           | See Eq (18)                            |
| $U$           | Velocity                               |
| $u$           | Velocity in boundary layer             |
| $V_0$         | Velocity at departure from eddy        |
| $V_T$         | Thermophoretic velocity                |
| $x$           | Distance along blade                   |
| $y$           | Distance normal to blade               |
| $\tau_w$      | Boundary shear stress                  |
| $\varepsilon$ | Eddy diffusivity ( $= \varepsilon_p$ ) |
| $\mu$         | Fluid viscosity                        |
| $\rho$        | Fluid density                          |
| $\rho_p$      | Particle density                       |
| $\nu$         | Kinematic viscosity                    |
| $\delta$      | Boundary layer thickness               |

### Dimensionless numbers

|                            |                        |
|----------------------------|------------------------|
| $C_* = \frac{C}{C_\infty}$ | Particle concentration |
| $K_* = \frac{N}{C_* u_*}$  | Deposition velocity    |

|  |                         |
|--|-------------------------|
| $r_* = \frac{ru_*}{\nu}$               | Particle radius         |
| $S_* = \frac{su_*}{\nu}$               | Stopping distance       |
| $u_* = (\tau_w/\rho)^{1/2}$            | Shear velocity          |
| $M = \frac{U}{U_A}$                    | Mach number             |
| $Pr = \frac{\mu C_p}{k}$               | Prandtl number          |
| $Re_c = \frac{U_\infty c}{\nu}$        | Passage Reynolds number |
| $Re_d = \frac{U_{\infty 1} d}{\nu}$    | Droplet Reynolds number |
| $Sc = \frac{\nu}{D}$                   | Schmidt number          |
| $Sh = \frac{Kx}{D}$                    | Sherwood number         |
| $Sto = \frac{\rho_p d^2 V_p}{18\mu c}$ | Stokes number           |

### Subscripts

|          |                       |
|----------|-----------------------|
| A        | Acoustic              |
| a        | Atmosphere            |
| c        | Concentration         |
| D        | Diffusion             |
| h        | Hydrodynamic          |
| p        | Particle              |
| r        | Residual              |
| w        | Wall                  |
| x        | Flow-wise             |
| y        | Perpendicular to flow |
| 1        | Blade inlet           |
| 2        | Blade outlet          |
| $\infty$ | Free stream           |

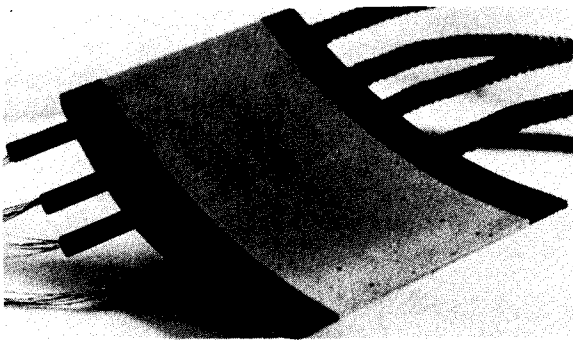


Fig 2 Blade assembly with heating connections and thermocouple leads. Black surface spots near the blade outlet are filled holes above constructional screws

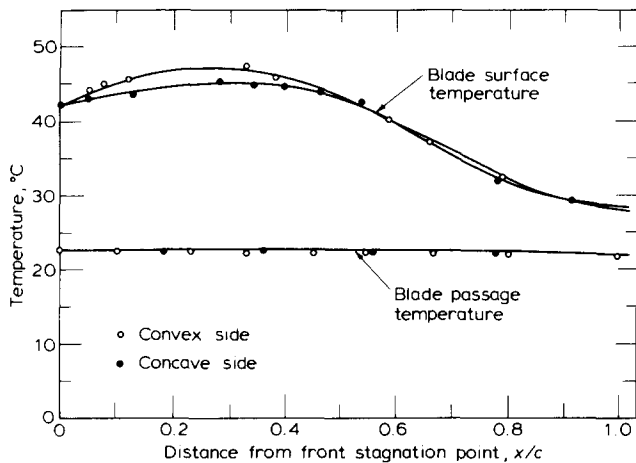


Fig 3 Temperature distribution on and around test blade surface ( $U_1 = 13.0$  m/s; atmospheric temperature,  $T_a = 21$  °C).

To obtain acceptable results, and to allow for urban air background contamination reaching 50–90% of the total mass deposited, all tests were repeated from two to four times.

### Temperature distribution around test blade surface

Families of temperature readings on the blade surfaces were taken for each set of conditions: (a)  $U_1 = 13.0$  m/s, gas pressure 30 mm water,  $T_a = 21$  °C. Corresponding values are for (b) 11.2, 30, 21.5 and for (c) 9.5, 30, 21.5. The curves are closely similar and those for case (a) are shown in Fig 3. Blade surface temperature increases from the leading edge to the point  $x/c = 0.4$  which is the position of maximum heating, after which the temperature declines as the trailing edge is approached. This is a consequence of the different sizes of the air chambers. From  $x/c > 0.90$  there is no room for an air chamber within the profile.

### Heat transfer

#### Laminar boundary layer

The hydrodynamic boundary layer momentum equation:

$$\left(\frac{\tau_w \theta}{\mu U}\right) = \frac{U}{2} \frac{d}{dx} \left(\frac{\theta^2}{\nu}\right) + \frac{\theta^2}{\nu} (H+2) \frac{dU}{dx} \quad (1)$$

is calculated first. If  $Pr$  is known for the fluid the thermal boundary layer thickness can then be found. Thence the local temperature gradient, heat transfer rate and  $Nu$  can be found.

Laminar boundary layer calculations were started from the forward stagnation point and transition occurred at  $x/c = 0.15$  (concave surface) and  $x/c = 0.67$  (convex surface). The heat transfer has a peak value at the stagnation point given by<sup>4</sup>:

$$\frac{Nu}{\sqrt{Re_2}} = 1.14 \left[\frac{c}{2R}\right] \left[\frac{U_1}{U_2}\right]^{Pr^{0.4}} \quad (2)$$

and the temperature gradient is given by:

$$\left(\frac{dT}{dy}\right)_{y=0} = \frac{Nu}{c} (T_w - T_\infty) \quad (3)$$

#### Turbulent boundary layer

The starting point for the analysis is the Von Karman Universal Velocity Profile which divides the turbulent boundary layer into three zones:

- |                   |   |       |
|-------------------|---|-------|
| 1. $y_* < 5$      | Laminar sublayer with transfer due to molecular processes | } (4) |
| 2. $5 < y_* < 30$ | Buffer zone with molecular and eddy transfer              |       |
| 3. $30 < y_*$     | Turbulent zone with eddy transfer dominant                |       |

Using the Fourier Law for the laminar sublayer and the Reynolds analogy for the buffer zone and turbulent zone in turn, the heat transferred for each zone may be stated in terms of the temperature difference across the zone. Considering the full boundary layer, the heat transfer equation becomes:

$$\frac{Nu}{(Re_2)^{1/2}} = \frac{(U/U_2)(Re_2)^{1/2}}{(Z/Pr)[Z + 5(Pr - 1)]} + \frac{1}{5 \ln \{1 + \frac{5}{6}(Pr - 1)\}} \quad (5)$$

where  $Z = U/u_*$  is a skin friction parameter. Eq. (5) may be written as

$$\frac{Nu}{(Re_2)^{1/2}} = \frac{-(U/U_2)(Re_2)^{1/2}}{G(Z, Pr)} \quad (6)$$

where  $G(Z, Pr)$  denotes a function of  $Z$  and  $Pr$  which has been plotted by Wilson and Pope<sup>4</sup>. As before, the temperature gradient is given by:

$$\left(\frac{dT}{dy}\right)_{y=0} = \frac{Nu}{c} [T_w - T_\infty] \quad (3)$$

The distribution of heat transfer was calculated for each set of the conditions given above and was similar

for all cases. One case is shown in Fig 4 and includes experimentally determined values of heat transfer. Results are displayed as the logarithm of the temperature gradient versus the dimensionless distance from the trailing edge, this method being chosen because temperature gradients are important for calculation of thermophoretic velocity.

### Particle deposition on blade surfaces

The seven agencies which may act, singly or together, to deposit particles on surfaces have been described briefly elsewhere<sup>3</sup>. In the present context, as in the earlier work<sup>3</sup>, only diffusion processes are operative.

Both the experimental method for the determination of deposition employed here<sup>1,5</sup> and the theory for diffusive deposition on surfaces<sup>5,7</sup> have been discussed at some length elsewhere and only a brief description is included here for the sake of continuity.

### Laminar boundary layer

The treatment is standard and leads to the relation:

$$\frac{N}{C_\infty D} = 0.332 Re_x^{1/2} Sc^{1/3}/x \quad (7)$$

which may be written in the alternative form:

$$Sh = \frac{Kx}{D} = 0.332 Re_x^{1/2} Sc^{1/3} \quad (8)$$

### Turbulent boundary layer

#### Molecular diffusion associated with eddy diffusion

The dimensionless form of the diffusion equation for this case is:

$$N = \left( \frac{D}{\nu} + \frac{\varepsilon}{\nu} \right) \frac{dC_*}{dy_*} \quad (9)$$

The values of  $\varepsilon$  are taken from Lin *et al*<sup>6</sup>:

$$\begin{aligned} \frac{\varepsilon}{\nu} &= \left[ \frac{y_*}{14.5} \right]^3 & \text{for } y_* < 5 \\ \frac{\varepsilon}{\nu} &= \frac{y_*}{5} - 0.959 & \text{for } 5 < y_* < 30 \\ \varepsilon &= \nu & \text{for } y_* > 30 \end{aligned} \quad (10)$$

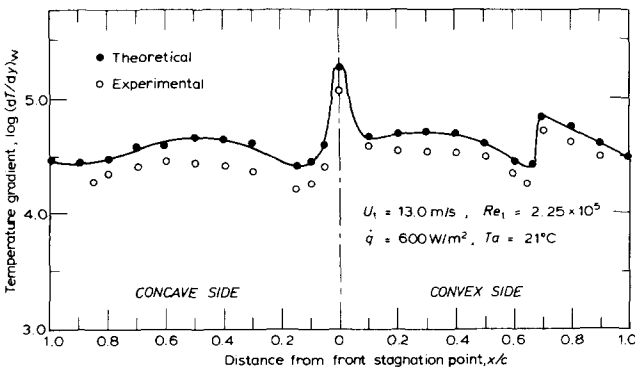


Fig 4 Variation of rate of heat transfer on blade surfaces

Eq (9) may be integrated over the full width of the boundary layer using Eq (10) for the appropriate regions and taking  $C_* = 0$  when  $y_* = r_*$  thus giving the concentration distribution. It is found, however, that for particles of size  $d = 0.01 - 1.0 \mu\text{m}$ , ie the range for turbine nucleation fogs, more than 90% of the concentration drop occurs within the boundary sub-layer. This permits simplification of the deposition Eq (9) to:

$$K_* = \left[ \frac{D}{\nu} + \left( \frac{y_*}{14.5} \right)^3 \right] \frac{dC_*}{dy_*} \quad (11)$$

which, upon integration gives:

$$14.5 \left( \frac{D}{\nu} \right)^{2/3} \left\{ \frac{1}{6} \ln \frac{(1 + \phi_*)^2 (1 - \psi_* + \psi_*^2)}{(1 + \psi_*)^2 (1 - \phi_* + \phi_*^2)} + \frac{1}{\sqrt{3}} \left\{ \tan^{-1} \frac{2\phi_* - 1}{\sqrt{3}} - \tan^{-1} \frac{2\psi_* - 1}{\sqrt{3}} \right\} \right\} \quad (12)$$

where

$$\begin{aligned} \phi_* &= \frac{1}{2.9 \left( \frac{D}{\nu} \right)^{1/3}} \\ \psi_* &= \frac{r_*}{14.5 \left( \frac{D}{\nu} \right)^{1/3}} \end{aligned}$$

#### Eddy diffusion followed by eddy impaction

Larger particles are not subject to molecular diffusion. Abandoned by the entraining eddy at the edge of the sublayer, a large particle may possess enough momentum to travel independently to the surface. For such particles Eq (11) reduces to:

$$K_* = \left[ \frac{y_*}{14.5} \right]^3 \frac{dC_*}{dy_*} \quad (13)$$

Integrating within the limits  $C_* = 1$  for  $y_* = \infty$  and  $C_* = 0$  for  $y_* = S_*$  where  $S_* = su_*/\nu$  and  $s = V_0 t$  gives the velocity of deposition due to eddy impaction as:

$$K_* = S_*/1525 \quad (14)$$

#### The diffusion layer

To distinguish between the eddy diffusion/molecular diffusion regime, where the process is controlled by  $D$  and  $\varepsilon$  and the eddy diffusion/eddy impaction regime which is controlled by  $\varepsilon$  and  $s$ , we employ the concept of the 'diffusion layer'. The regime boundary is deemed to be located where, say,  $\varepsilon = 5D$  and from Eq (11) the diffusion layer may be shown to have the dimensionless thickness:

$$y_D = \frac{24.8}{u_*} \left( \frac{D}{\nu} \right)^{1/3} \quad (15)$$

To predict deposition on the blade leading edge, use was made of a method proposed by Pich<sup>8</sup> and described by El-Shobokshy<sup>5</sup>.

## Thermophoresis

Any particle entrained in a fluid and subject to a thermal gradient is acted upon by a thermophoretic force tending to propel it down the gradient. This subject has been widely studied since first described by Tyndall<sup>9</sup>. Thermophoretic effects are sensitive to particle size. Small particles have been studied by, among others, Deryagin and Bakanov<sup>10</sup>, Waldmann<sup>11</sup> and Mason and Chapman<sup>12</sup>, and large particles by, among others, Epstein<sup>13</sup> and Brock<sup>14</sup>. Here, use was made of the expression due to Brock<sup>14</sup>:

$$V_T = -1.5 \frac{\mu}{\rho T} \frac{(k_g + C_t k_p l/r)}{(1 + 3Fl/r)(2k_g + k_p + 2C_t l/r)} \cdot \left( \frac{dT}{dy} \right) \quad (16)$$

A liquid particle subject to a local temperature higher than the saturation value for the pressure will be subject to evaporation. The heating of turbine blades has also been employed primarily in an attempt to evaporate entrained and deposited liquid with a view to the suppression of subsequent erosion<sup>15-17</sup>. The propriety of using a solid particle, immune from phase change, for these studies, will be discussed later.

## Thermophoresis in diffusion through a boundary layer

Adjacent to a heated surface the effect of thermophoresis is a tendency to propel a particle away from the surface. By contrast, the existence of a concentration gradient tends to cause the deposition of particles. The actual deposition on a heated turbine blade will be due to the net effect and the mass transfer will be given by:

$$N = D \frac{dC}{dy} + V_T C \quad (17)$$

where  $V_T$  is negative for this case. Eq (17) may be integrated with the boundary conditions  $C = 0, y = 0$ ;  $C = C_0, y = \delta_C$  where  $\delta_C = 0.3425 \delta_h (D/\nu)^{1/3}$  is the concentration boundary layer thickness and  $\delta_h$  the hydrodynamic boundary layer thickness. Solving:

$$\int_0^{C_0} \frac{dC}{N - V_T C} = \int_0^{\delta_C} \frac{dy}{D}$$

gives:

$$\left( 1 - \frac{V_T}{K_r} \right) = e^{-t} \quad \text{or} \quad K_r = \frac{V_T}{1 - e^{-t}} \quad (18)$$

where  $K_r$  is the residual (net) deposition velocity and  $t = (V_T \delta_C)/D$  is the ratio: thermophoretic force/diffusive force.

## Thermophoresis in diffusion through a turbulent boundary layer

As in the case of the laminar boundary layer thermophoresis acts so as to tend to reduce the deposition.

Eq (17) may be modified for this case and in its dimensionless form reads:

$$K_* = \left( \frac{D}{\nu} + \frac{\varepsilon}{\nu} \right) \frac{dC_*}{dy_*} + V_{T*} C_* \quad (19)$$

As explained above the expression for eddy diffusivity in the laminar sublayer may be used for  $\varepsilon/\nu$ . The boundary conditions for integration are  $C_* = 0, y_* = r_*$ ;  $C_* = 1, y_* = 5$ , hence:

$$\int_0^1 \frac{dC_*}{(K_* - V_{T*} C_*)} = \int_0^5 \frac{dy_*}{\frac{D}{\nu} + \left[ \frac{y_*}{14.5} \right]^3}$$

which gives:

$$\left[ \frac{1}{V_{T*}} \ln (K_* - V_{T*} C_*) \right]_0^1 = E$$

where:

$$E = 14.5 \left( \frac{\nu}{D} \right)^{2/3} \left[ \frac{1}{6} \ln \frac{(1 + \phi_*)^2 (1 - \psi_* + \psi_*^2)}{(1 + \psi_*)^2 (1 - \phi_* + \phi_*^2)} + \frac{1}{\sqrt{3}} \left( \tan^{-1} \frac{2\phi_* - 1}{\sqrt{3}} - \tan^{-1} \frac{2\psi_* - 1}{\sqrt{3}} \right) \right]$$

and where:

$$\phi_* = \frac{1}{2.9 \left( \frac{D}{\nu} \right)^{1/3}} \quad \text{and} \quad \psi_* = \frac{r_*}{14.5 \left( \frac{D}{\nu} \right)^{1/3}}$$

Re-arranging leads to:

$$K = K_r = \frac{V_T}{(1 - e^{-V_T E})} \quad (20)$$

where  $K_r$  is the residual velocity of deposition.

It should be borne in mind that in addition to diffusive and thermophoretic forces, gravitational forces are also present. Furthermore, since blade passages are curved, centrifugal forces are present. However, the nucleation fog size is only in the range 0.01–1.0  $\mu\text{m}$  diameter and the effects of sedimentation and inertia are very small. Further information on the size and physical behaviour of turbine fog droplets is given by Gyarmathy<sup>18</sup>.

## Experimental studies on deposition

The methods used to determine the actual deposition have been outlined above and described in detail elsewhere<sup>7</sup>.

Datum tests with unheated blades were made using particle populations having respective mass median diameters of 0.05, 0.13, 0.185 and 0.25  $\mu\text{m}$ . For each population, tests were made for blade Reynolds numbers ( $Re_1$ ) of  $1.65 \times 10^5$ ,  $1.95 \times 10^5$  and  $2.25 \times 10^5$  corresponding to cascade inlet velocities of 9.5, 11.2 and 13.0 m/s. The general pattern of distribution was the same for all combinations of conditions and

Figs 5 and 6 show results for each extreme case. All results are recorded by Davies<sup>19</sup>.

Tests with heated blades were conducted using the same range of particle size and flow conditions. The effect of heating is displayed as a percentage reduction in deposition; Figs 7 and 8 to Figs 5 and 6 respectively. The values of heat input per unit area are  $600 \text{ W/m}^2$  and  $626 \text{ W/m}^2$ . This is a low heat intensity and suggests that a rotor blade ring at risk may be capable of protection at a very modest cost.

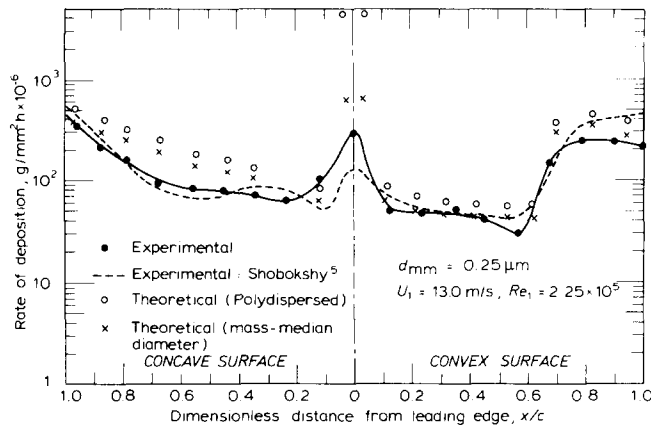


Fig 5 Distribution of particle deposition on blade surfaces (unheated blades)

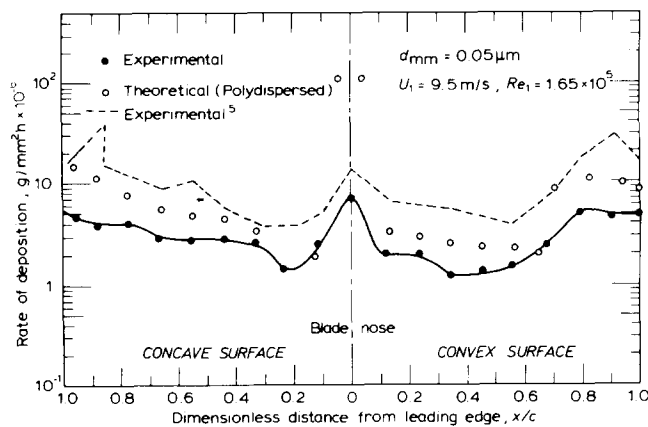


Fig 6 Distribution of particle deposition on blade surfaces (Heated blades, except Ref 5)

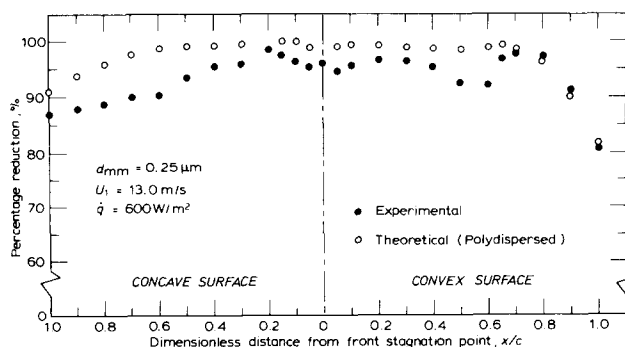


Fig 7 Percentage reduction in particle deposition due to thermophoresis on blade surfaces

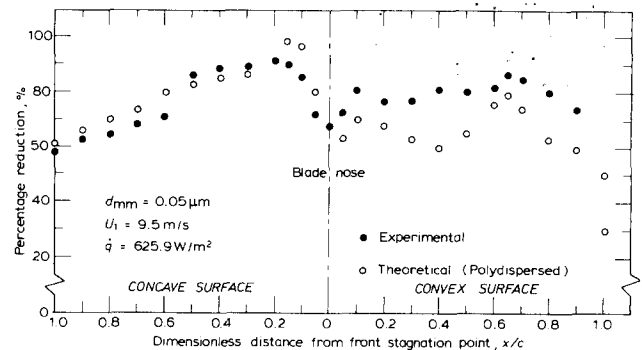


Fig 8 Percentage reduction in particle deposition due to thermophoresis on blade surfaces

### Conclusions and comments

Experimental work with highly dispersed aerosols demands great skill and, because of the likelihood of contamination, scrupulous cleanliness must be observed. To obtain acceptable results and to allow for urban air background contamination reaching 50–90% of the total mass deposited, all tests were repeated from two to four times.

Considering the results as a whole, the following main conclusions were found:

- The total mass of particles deposited on the concave surface exceeded that deposited on the convex surface by an average of 15%. This is because approximately 70% of the concave surface, compared with 35% of the convex surface, is subject to turbulent mass transfer which is generally higher than laminar mass transfer.
- For each particle size, the total mass deposition on the heated blade decreased with decreasing inlet velocity. This is partly because deposition rate is thus in agreement with theoretical prediction but also because the heat input was constant at all inlet velocities and so, at the lower velocity values, thermophoretic forces are more intense.
- Deposition was reduced by 30–90% at most positions on the heated blades. Deposition on the heated blade nose was still high but, compared to the isothermal value, there was an average reduction of about 70%. This is because at the nose the temperature gradient and hence particle repulsion was very large.
- Due to the difficulty of heating the trailing edge sufficiently the percentage reduction in deposition fell towards the passage exit.

The predictive value of the above method when applied to fog droplets within the L.P. turbine guide blade depends upon two major criteria:

1. The adequate modelling in air of the relevant dimensionless groups concerned with diffusive deposition in steam<sup>1,5,7</sup>. It has been shown that the groups having significance are  $Sto$ ,  $Re_c$ ,  $Re_d$ ,  $Sc$ ,  $M$ . It can be shown that  $Re_c$ ,  $Re_d$  and  $Sc$  can be acceptably modelled. The Mach Number  $M$  cannot be modelled but it has long been acceptable to relax this constraint in air-test studies on turbine blades. For studies on diffusive deposition as distinct from inertial deposition  $Sto$  is not significant.

2. The most serious criticism of the above method arises from the fact that solid particles undergo no change of phase whereas fog droplets in proximity to a heated blade surface are subject to evaporation, thus diminishing in size or even disappearing completely. As diffusion and thermophoresis are sensitive to size, valid modelling may be prejudiced. The magnitude of the error incurred depends upon the thermal relaxation time of the drop, ie the time needed to attain thermal equilibrium with its surroundings. Pertinent here are (i) the time of transit of the droplet through the nozzle which may be much shorter than the evaporation time; (ii) the initial size of the droplet, and (iii) the heat input which governs the superheat within the boundary layer and the magnitude of the temperature gradient.

It is evident that the behaviour of the largest fog droplets, 1  $\mu\text{m}$  diameter, will be most nearly described by the above methods but the smallest droplets, 0.01  $\mu\text{m}$  diameter, will have a different pattern of behaviour. To shed further light on this difficult subject, an attempt is now being made to analyse from theory the coupled boundary layer effects of diffusion, thermophoresis and phase change upon a suspended fog droplet population. Each of these phenomena, taken singly, is well understood.

### Acknowledgements

This work was done in the Wet Steam Laboratory, Department of Mechanical Engineering, University of Liverpool during the period 1976–1980. The apparatus was provided by the (then) Science Research Council, London. J. B. Davies was supported by the Government of Sierra Leone.

We are grateful to Mr. P. Devenish for help with the Electron Microscopy, Mr T. Canavan for manufacturing the blades, Mr E. Hughes for help with the experimental work and Dr J. W. Cleaver for interest and advice.

### References

1. Ryley D. J. and Parker G. J. Equipment and techniques for studying the deposition of sub-micron particles on turbine blades. *Proc. Instn. Mech. Engrs.*, 1969–70, **184**, Pt. (3c), 45–53
2. Parker G. J. and Lee P. Studies of the deposition of sub-micron particles on turbine blades. *Proc. Instn. Mech. Engrs.*, 1972, **186**, 38/72, 519–526
3. Ryley D. J. and El-Shobokshy M. S. The deposition of fog droplets by diffusion onto steam turbine guide blades. *Sixth Int. Heat Transfer Conf., Toronto, Aug. 7–11, 1978, Paper EC-14*, 85–90
4. Wilson D. G. and Pope J. A. Convective heat transfer to gas turbine blade surfaces. *Proc. Instn. Mech. Engrs.*, 1954, **168**, 861–874
5. El-Shobokshy M. S. Diffusional deposition of fog droplets onto low-pressure steam turbine guide blades at off-design conditions. *Ph.D. Thesis*, 1975, *University of Liverpool*
6. Lin C. S., Moulton R. W. and Putnam G. L. Mass transfer between solid wall and fluid streams. *Ind. Engr. Chem.*, 1953, **49**(1), 636–646
7. Davies C. N. Brownian deposition of aerosol particles from turbulent flow through pipes. *Proc. Roy. Soc. Series A*, 1966, **290**, 557–562
8. Pich J. A note on diffusive deposition of aerosols on a cylinder. *J. Aerosol Sci.*, 1970, **1**, 17–19
9. Tyndall J. On dust and disease. *Proc. Roy. Instn.*, 1870, **6**, 1
10. Deryagin B. V. and Bakanov S. P. Theory of diffusion of aerosols. *Dokl. Akad. Nauk., S.S.S.R.*, 1957, **117**, 959–962
11. Waldmann L. Über die Kraft eines inhomogenen Gases auf kleine suspendierte Kugeln. *Z. Naturf.*, 1959, **14a**, 588–599
12. Mason E. A. and Chapman S. Motion of small suspended particles in non-uniform gases. *J. Chem. Phys.*, 1962, **36**, 627–632
13. Epstein P. S. Zur Theorie des Radiometers. *Z. Physik*, 1929, 537–563
14. Brock J. R. On the theory of thermal forces acting on aerosol particles. *J. Colloid Sci.*, 1962, **17**, 768–780
15. Engelke W. Operating experience of wet steam turbines in *Two-Phase Steam Flow in Turbines and Separators* (eds. M. J. Moore and C. H. Sieverding) McGraw-Hill, 1976, 291–315
16. Konorski A. Steam drying in condensing turbines by internal preheating method utilising its own steam. (*Paper in Polish, Summary in English*). IMP. PAN, Gdansk, 1962, 63–120
17. Konorski A., Janowski T. and Prokopowicz J. Heat exchange and evaporation of water film on heated guide vanes of steam turbines. (*Paper in Polish, Summary in English*). IMP. PAN, Gdansk, 1971, 129–159
18. Gyarmathy, G. Basic notions (*Chapter 1*) and Condensation in flowing steam (*Chapter 3*) in *Two-Phase Steam Flow in Turbines and Separators* (eds. M. J. Moore and C. H. Sieverding) McGraw-Hill, 1976
19. Davies J. B. The effect of thermophoresis on the deposition of fog droplets on low-pressure turbine fixed blades. *Ph.D. Thesis*, Dept. of Mechanical Engineering, The University of Liverpool, 1980